Quantum Monte Carlo approaches to the Harmonic Oscillator and the Heisenberg model

Inácio, João[1] and Aarstein, Daniel[1]

[1]*Department of Physics, University of Oslo, Norway, Sem Sælands vei 24, 0371 Oslo*

(Dated: August 29, 2022)

In this work, we study the quantum harmonic oscillator and the Heisenberg model through different path integral Monte Carlo approaches. For the harmonic oscillator system, we use the well-known imaginary-time path integral method and for the Heisenberg model the Stochastic Series Expansion method is used. An implementation of Stochastic Series Expansion is also developed for the 1D and 2D anisotropic Heisenberg model with an applied filed in the z direction. We study the first excitation level of the harmonic oscillator model and the effect of magnetic anisotropy and external field on the Heisenberg model. The first excited energy level for the harmonic oscillator system was found to be given by $\Delta E = 1.06616$ which somewhat differs from Lepage's notes on the subject [1]. Part of the code and results used in this report can be found at this `https://github.com/jgci2000/FYS4411-pimc` GitHub repository. The Stochastic Series Expansion implementatiom may be found at `https://github.com/jgci2000/SSE`.

In this project, we aim to build a code for the imaginary-time path integral method to study a system with one atom trapped in an harmonic oscillator potential and a code to simulate the anisotropic Heisenberg model in a magnetic field trough the Stochastic Series Expansion method (SSE) [2, 3]. We also wish to study the effects of magnetic anisotropy and external field on the Heisenberg interaction.

Both the imaginary-time path integral method and the SSE, rely on the Monte Carlo method to sample a determined configuration space with a given weight probability. In the case of the path integral method, this weight is given by the exponential of the Euclidean action, while on the SSE method, we use a series of diagonal and loop-operator updates, weighted by the Hamiltonian term, to sample the configuration space. Both of these method belong to the Path Integral Monte Carlo class of method, but use different approaches. In the imaginary-time path integral method we perform a so-called Wick rotation in to imaginary time and discretize the imaginary-time axis to sample the possible paths weighted by the Euclieand action. In SSE, we perform a high-temperature expansion of the quantum mechanical partition function and sample an operator space given by the Hamiltonian operators.

Notes on how to measure expectation values of operators in the SSE picture and an application of the SSE method to the Heisenberg model are also given. In the end we study the first excitation energy of the harmonic oscillator model and the effect of magnetic anisotropy and external field on the Heisenberg model.

HEISENBERG MODEL

The $S = 1/2$ Heisenberg Model is a quantum model for magnetism proposed by Werner Heisenberg. The model describes a system of N quantum spin particles arranged on a d-dimensional lattice, where only near-neighbour interactions are considered. The Hamiltonian can be written as

$$H = J \sum_{\langle i,j \rangle} \boldsymbol{S}_i \cdot \boldsymbol{S}_j,$$

where $\boldsymbol{S}_i$ is the total spin operator for particle i, and the sum is conducted over all neighbouring sites i and j. J is called the coupling constant, has units of energy, and describes the interaction strength between two neighbouring particles. If $J > 0$, the system will have an antiferromagnetic behaviour, where disalignment between neighbouring spins is favoured, while with $J < 0$, a ferromagnetic behaviour will prevail, favouring alignment between neighbouring spins.

In this work we will focus on the antiferromagnetic Heisenberg model, thus consider $J > 0$. We will also consider the complete basis $|\alpha\rangle$, with

$$|\alpha\rangle = \left|S_1^z S_2^z \dots S_N^z\right\rangle.$$

Considering the following relations,

$$\boldsymbol{S} = S^x \boldsymbol{e}_x + S^y \boldsymbol{e}_y + S^z \boldsymbol{e}_z;$$
$$S^x = \frac{1}{2}\left(S^+ + S^-\right); \quad S^y = \frac{1}{2i}\left(S^+ - S^-\right);$$

we can rewrite the expression for the Hamiltonian as

$$H = J \sum_{\langle i,j \rangle} \left(S_i^z S_j^z + \frac{1}{2}\left(S_i^+ S_j^- + S_i^- S_j^+\right)\right).$$

In a more general note, we can add spin anisotropy Δ along the z-axis and an external magnetic field h aligned with the z-axis.

$$\begin{aligned} H &= J \sum_{\langle i,j \rangle} \left[\Delta S_i^z S_j^z + \frac{1}{2}\left(S_i^+ S_j^- + S_i^- S_j^+\right)\right] - h \sum_{i=0}^{N} S_i^z \\ &= J \sum_{\langle i,j \rangle} \left[\Delta S_i^z S_j^z - \frac{h}{2J}\left(S_i^z + S_j^z\right) + \frac{1}{2}\left(S_i^+ S_j^- + S_i^- S_j^+\right)\right] \end{aligned}$$

It is more convenient to change the sum over neighbouring sites i and j to a sum over bonds b, where we can recover the sites by $i(b)$ and $j(b)$. In a d-dimensional system with N particles there are $N_b = dN$ bonds. Then,

$$H = J\sum_{b=1}^{N_b}\left[\Delta S^z_{i(b)}S^z_{j(b)} - \frac{h}{2J}\left(S^z_{i(b)}+S^z_{j(b)}\right)+\frac{1}{2}\left(S^+_{i(b)}S^-_{j(b)}+S^-_{i(b)}S^+_{j(b)}\right)\right]$$

We can also divide the sum in to two terms, the diagonal terms $H_{1,b}$ or off-diagonal terms $H_{2,b}$, where

$$H_{1,b} = C - \Delta S^z_{i(b)}S^z_{j(b)} + \frac{h}{2J}\left(S^z_{i(b)}+S^z_{j(b)}\right);$$
$$H_{2,b} = \frac{1}{2}\left(S^+_{i(b)}S^-_{j(b)}+S^-_{i(b)}S^+_{j(b)}\right).$$

Then,

$$H = -J\sum_{b=1}^{N_b}\left(H_{1,b}-H_{2,b}\right)+JN_bC.$$

Here a constant $C = C_0+\varepsilon$ was added such that the diagonal terms in the Hamiltonian are positive, in order to avoid sign-problems [4] in the Monte-Carlo sampling routine. All of the non-zero matrix elements of $H_{1,b}$ are

$$\langle\uparrow\uparrow|H_{1,b}|\uparrow\uparrow\rangle = C - \frac{\Delta}{4}+\frac{h}{2J};$$
$$\langle\downarrow\downarrow|H_{1,b}|\downarrow\downarrow\rangle = C - \frac{\Delta}{4}-\frac{h}{2J};$$
$$\langle\uparrow\downarrow|H_{1,b}|\uparrow\downarrow\rangle = \langle\downarrow\uparrow|H_{1,b}|\downarrow\uparrow\rangle = C+\frac{\Delta}{4}.$$

This means that $C \geq \Delta/4+h/(2J)$, then we define

$$C_0 = \Delta/4+h/(2J),$$

and $\varepsilon \geq 0$. Then all of the non-zero matrix elements of the Hamiltonian are

$$\langle\uparrow\uparrow|H_{1,b}|\uparrow\uparrow\rangle = \frac{h}{J}+\varepsilon;$$
$$\langle\downarrow\downarrow|H_{1,b}|\downarrow\downarrow\rangle = \varepsilon;$$
$$\langle\uparrow\downarrow|H_{1,b}|\uparrow\downarrow\rangle = \langle\downarrow\uparrow|H_{1,b}|\downarrow\uparrow\rangle = \frac{\Delta}{2}+\frac{h}{2J};$$
$$\langle\uparrow\downarrow|H_{2,b}|\downarrow\uparrow\rangle = \langle\downarrow\uparrow|H_{2,b}|\uparrow\downarrow\rangle = \frac{1}{2}.$$

PATH INTEGRALS

The path integral formalism for quantum mechanics was finalized by Richard Feynman in the late 1940's after building on ideas put forth by Norbert Wiener and Paul Dirac. It has proven to be an equally valid way of describing quantum mechanics as the wavefunction formalism where the wavefunction is the solution of the Schrödinger equation. The overarching idea is to extend the concept of least action from classical mechanics (classical field theory) into quantum mechanics (quantum field theory).

In classical mechanics the action is given by the definite integral over the Lagrangian, which again is defined by the kinetic energy minus the potential energy. That is

$$S[x] = \int_{t_i}^{t_f}\mathscr{L}(x,\dot{x})dt$$

where

$$\begin{aligned}\mathscr{L}(x,\dot{x}) &= K - V\\ &= \frac{1}{2}m\dot{x}^2 - V(x)\\ &= \frac{p^2}{2m} - V(x)\end{aligned}$$

The time evolution of the system will then be given by the $x(t)$ which minimizes the action.

Due to the non-deterministic nature of quantum mechanics, the time evolution of the system is not solely given by the path that minimizes the action. However, the action plays an important role as the probability of a given path being taken is now weighted by the action. In order to obtain the time evolution of the system one simply has to evaluate every single possible path the system might take, and give them probabilistic weights proportional to their action. The resulting integral over all possible paths is what is known as the path integral formalism.

The evolution from state $|x_i,t_i\rangle$ to $|x_f,t_f\rangle$ is then given by

$$\begin{aligned}&\langle x_f,t_f|\exp\left[\frac{-iH(t_f-t_i)}{\hbar}\right]|x_i,t_i\rangle =\\ &= \int_{x_i}^{x_f}\mathscr{D}[x(t)]\exp\left[\frac{i}{\hbar}\int_{t_i}^{t_f}dt\mathscr{L}(x,\dot{x})\right]\\ &= \int_{x_i}^{x_f}\mathscr{D}[x(t)]\exp\left[\frac{i}{\hbar}S[x]\right]\end{aligned}$$

where $\mathscr{D}$ indicated the integral over all possible $x(t)$ such that $x(t_i) = x_i$ and $x(t_f) = x_f$, $\mathscr{L}(x,\dot{x})$ is the classical Lagrangian, i is the imaginary unit and $\hbar$ is the reduced Planck constant.

We will now let the system undergo a *Wick rotation*. That is, we let $t \to it$. This is equivalent to changing the space-time geometry from Lorentzian to Euclidean. This has two important consequences.

Firstly, the integral over the classical Lagrangian changes

$$\int_{t_i}^{t_f}dt\mathscr{L}(x,\dot{x}) \to \int_{t_i}^{t_f}idt\mathscr{L}(x,\dot{x})$$

which, secondly, leads to

$$\int_{x_i}^{x_f}\mathscr{D}[x(t)]\exp\left[\frac{i}{\hbar}S[x]\right] \to \int_{x_i}^{x_f}\mathscr{D}[x(t)]\exp\left[\frac{-S_E[x]}{\hbar}\right]$$

where $S_E[x]$ is the Euclidean action defined as

$$S_E[x] = S_E(x,\dot{x}) = \int \left[\frac{1}{2}m|\dot{x}(t)|^2 + V(x)\right]dt$$

Note the absolute length of the $\dot{x}$ and the sign change of the potential. As noted by Lepage [1], the Wick rotation lends itself better for numerical work since the integrands in the Euclidean action do not oscillate wildly in sign.

Discretizing the Path Integral

Splitting the imaginary time into N equidistant time steps we have

$$t_j = t_i + ja \quad \text{for} \quad j = 0,1,\ldots,N$$

where a is the grid spacing defined as

$$a \equiv \frac{t_f - t_i}{N}$$

Using this we can generate a path, or configuration, for our path integral. That is, the path x is now given by the discrete values

$$\begin{aligned} x &= \{x(t_0), x(t_1), \ldots, x(t_{N-1})\} \\ &= \{x_0, x_1, \ldots, x_{N-1}\} \end{aligned}$$

The path integral is now approximated by taking the integral over all possible values for the different x_i's. That is, for fixed endpoints, given by

$$\int \mathscr{D}[x(t)] \to A \int_{-\infty}^{\infty} dx_1 dx_2 \ldots dx_{N-1}$$

where A is an appropriate normalization factor (which will not be necessary in this project).

Note that this is a $N-1$ dimensional integral, which by traditional means would be unfeasible to calculate numerically.

Turning our attention back to the Euclidean action (henceforth denoted simply by S) and looking at the contribution from the time interval $t \in [t_j, t_{j+1}]$ we have

$$S_j[x(t)] \approx a\left[\frac{m}{2}\left(\frac{x_{j+1}-x_j}{a}\right)^2 + \frac{1}{2}\big(V(x_{j+1}) + V(x_j)\big)\right]$$

where we replace the potential with the average potential and make the approximation

$$\dot{x}(t) \approx \frac{x(t_{j+1}) - x(t_j)}{\Delta t} = \frac{x_{j+1} - x_j}{a}$$

The complete Euclidean action is then given as a sum of all the partial actions, in total

$$\begin{aligned} S[x(t)] &= \sum_{j=0}^{N-1} S_j[x(t)] \\ &= \sum_{j=0}^{N-1} a\left[\frac{m}{2}\left(\frac{x_{j+1}-x_j}{a}\right)^2 + \frac{1}{2}\big(V(x_{j+1}) + V(x_j)\big)\right] \\ &= \sum_{j=0}^{N-1}\left[\frac{m}{2a}\big(x_{j+1}-x_j\big)^2 + aV(x_j)\right] \end{aligned}$$

Because of the periodic boundary conditions, $x_0 = x_N$ and all the potentials are encountered twice, thus summing to one in total.

Note that the element x_j only is needed for calculating S_{j-1} and S_j. This makes it possible to gather the terms with j into one action, which will be used in the code as there now is no need to calculate S_{j-1} and S_j twice within the same update. The action for time interval j is then in the code given by

$$S_j[x(t)] = \frac{m}{a}x_j\big(x_j - x_{j-1} - x_{j+1}\big) + aV(x_j)$$

With an approximation to both the path integral itself and the action which determines the weight, everything needed to approximate the propagator is known.

With a known S we may calculate the correlation

$$\langle x(t_2)x(t_1)\rangle = \frac{\int \mathscr{D}[x(t)]x(t_2)x(t_1)e^{-S}}{\int \mathscr{D}[x(t)]e^{-S}}$$

From this it is clear to see that the normalization factor A, as previously stated, is not needed as were in practice dividing by the partition function of the system. Letting T be the total imaginary time and having $t = t_2 - t_1$ we may rewrite the above expression as

$$\langle x(t_2)x(t_1)\rangle = \frac{\sum e^{-E_n T}\,\langle E_n|\tilde{x}e^{-(H-E_0)t}\tilde{x}|E_n\rangle}{\sum e^{-E_n T}}$$

If we now let $T >> t$, that is only look at small differences in imaginary time, the ground state will completely dominate the term leading to the correlation term

$$G(t) = \langle x(t_2)x(t_1)\rangle = \langle E_n|\tilde{x}e^{-(H-E_0)t}\tilde{x}|E_n\rangle$$

the propagator from the ground state to the first excitation state then leads to

$$G(t) = |\langle E_0|\,\tilde{x}\,|E_1\rangle|^2 e^{-(E_1-E_0)t}$$

Evaluating $G(t)$ at $t = 0$ and $t = \Delta t$, then solving for $\Delta E = E_1 - E_0$ gives

$$\Delta E = \frac{1}{\Delta t}\ln\left(\frac{G(t)}{G(t+\Delta t)}\right)$$

The algorithm

General notes on the Monte Carlo method are given in project 1 [5], and will not be discussed.

Using the Monte Carlo method for numerical integration we approximate the path integral by randomly sampling different paths such that the periodic boundary conditions are kept. That is, every path is given by some

$$x^{(\alpha)} = \left\{x^{(\alpha)}(t_0), x^{(\alpha)}(t_1), \ldots, x^{(\alpha)}(t_{N-1})\right\}$$

For $\alpha = 1,2,\ldots,N_{cf}$, where every element in $x^{(\alpha)}$ is uniformly chosen between the value $-\varepsilon$ and ε, a parameter which we are free to choose. The Metropolis

method for accepting or rejecting a configuration is implemented with the condition $e^{-\Delta S[x^{(\alpha)}]} < \gamma$ where $\Delta S[x^{(\alpha)}] = S[x^{(\alpha)}] - S[x^{(\alpha-1)}]$ and γ is an uniformly distributed number between 0 and 1. Note that if $S[x^{(\alpha-1)}] > S[x^{(\alpha)}]$ then $\Delta S[x^{(\alpha)} < 0$ and $e^{-\Delta S[x^{(\alpha)}]} > 1$ so that a new configuration will never be accepted if the action isn't lowered.
For a large number of configurations, N_{cf}, the paths which result in lower action will then be sampled more often. This ensures a better approximation for the correlation $\langle x(t_2)x(t_1)\rangle$.

STOCHASTIC SERIES EXPANSION

Another approach to the same problem is to construct a configuration space suitable for Monte Carlo sampling by using the high-temperature Taylor expansion of the partition function Z,

$$Z = \mathrm{Tr}\Big\{e^{-\beta H}\Big\} = \sum_{n=0}^{\infty} \frac{(-\beta)^n}{n!} \mathrm{Tr}\{H^n\},$$

where $\beta = 1/T$ and H is the Hamiltonian. This approach was pioneered by Handscomb in the 1960s [6, 7], who developed a method for studying the $S = 1/2$ Heisenberg ferromagnet. This power-series representation of the partition function is convergent for finite lattices at finite β, thus, unlike the path integral approach, there are no approximations causing systematic errors. A distinct advantage of Stochastic Series Expansion over continuous-time path integral methods is the discrete nature of the configuration space, which can be sampled without any floating point operations.

General Formalism

By choosing a certain basis $\{|\alpha\rangle\}$, we get

$$Z = \mathrm{Tr}\Big\{e^{-\beta H}\Big\} = \sum_{\alpha}\sum_{n=0}^{\infty} \frac{(-\beta)^n}{n!} \langle\alpha| H^n |\alpha\rangle,$$

where the trace as been written as a sum over the diagonal matrix elements of the basis elements $\{|\alpha\rangle\}$. The main difference from the path integral formalism is that the number of time "slices", the expansion power n, is varying and for given n there are particle jumps at each slice. The new time "propagation" dimension is labeled by $p = 0, \ldots, n-1$.

Truncating the Taylor expansion of the partition function at $n = M$, we can construct a fixed-size sampling space by introducing unit operators I. Allowing for all possible locations of the unit operators in the product of M operators, we can define an operator string $S_M = S_0 S_1 \ldots S_{M-1}$, in which $S_i \in \{I, H_1, H_2\}$[1], and perform a summation over all of these sequences. Weighting these terms accordingly, we get

$$Z = \sum_{\alpha}\sum_{S_M} (-1)^{n_2} \frac{\beta^n (M-n)!}{M!} \langle\alpha| \prod_{i=0}^{M-1} S_i |\alpha\rangle,$$

where n is now the number of Hamiltonian operators H and n_2 is a lattice dependent constant. For a bipartite lattice [2], n_2 is even and for a non-bipartite lattice, n_2 is odd. In actual simulations, this cut-off M is automatically determined by the program, as discussed later, such that M exceeds the largest n ever sampled. Note that his truncation then does not introduce any detectable errors and should not be considered as an approximation. It can be shown [6, 7] that the average expansion order if given by $\langle n\rangle = \beta N_b |E_b|$, where $E_b = -\langle H_b\rangle$ (including the constant C, defined prior).

It is useful to define

$$|\alpha(p)\rangle = \prod_{i=0}^{p} S_i |\alpha\rangle,$$

as the propagated state by a fraction of the SSE operator string. Note that $|\alpha(p)\rangle$ and $\alpha(p+1)$ are either the same states, if S_p is a diagonal operator, or differ only by one pair of flipped spins, if S_p is an off-diagonal operator. Here it is also required that $|\alpha(0)\rangle = |\alpha(M)\rangle$, such that the boundary condition is satisfied.

It is also useful to define a weight function for the configurations $\{\alpha, S_M\}$,

$$W(\alpha, S_M) = (-1)^{n_2} \frac{\beta^n (M-n)!}{M!} \langle\alpha| \prod_{i=0}^{M-1} S_i |\alpha\rangle,$$

such that we can write $Z = \sum_{\alpha}\sum_{S_M} W(\alpha, S_M)$. Choosing carefully the string operators S_i to be positive, the weights W will be positive definite and we can use a Monte Carlo procedure to sample the terms $\{\alpha, S_M\}$ according to their relative weights. In the original version of the SSE method, there were two main types of sampling schemes: diagonal updates, where the identity operators are substituted by diagonal ones according to their relative weights H_1, and off- diagonal updates where pairs of diagonal operators are substituted by off-diagonal operators, to keep the time periodicity [3, 8]. A few years after, a new type of sampling off-diagonal operators was devised. This method is called the operator-loop update scheme, and follows a similar procedure as the Swendsen-Wang cluster algorithm [9]. In this work the diagonal and loop update schemes will be used. We will go more in depth in to the updating schemes when we apply the SSE representation to the Heisenberg model.

Measuring Operators

This section is based on [2]. For more mathematical detail one may visit said reference.

[1] Here it is assumed that the Hamiltonian can be separated in to a diagonal part H_1 and an off-diagonal part H_2, such that $H = H_1 + H_2$.

[2] Bipartite lattices are defined as direct sums of two sub lattices A and B so that each site is connected only to sites of the other sub lattice.

In a quantum statistical mechanical system, we can measure the thermal average of an operator A [9], as

$$\langle A\rangle = \mathrm{Tr}\Big\{Ae^{-\beta H}\Big\}.$$

In the SSE representation, we can express this thermal average as

$$\langle A\rangle = \frac{1}{Z}\sum_{\alpha}\sum_{S_M}(-1)^{n_2}\frac{\beta^n(M-n)!}{M!}\langle\alpha|A\prod_{i=0}^{M-1}S_i|\alpha\rangle$$

Some function $A(\alpha,S_M)$ can be found such that

$$\langle A\rangle = \frac{\sum_\alpha\sum_{S_M}A(\alpha,S_M)W(\alpha,S_M)}{\sum_\alpha\sum_{S_M}W(\alpha,S_M)}.$$

Then the thermal average of the operator A can be found by sampling the space $\{\alpha,S_M\}$. Defining $\langle\ldots\rangle_W$ as the arithmetic average with the configurations generated by the weight W, we can rewrite $\langle A\rangle$ as

$$\langle A\rangle = \langle A(\alpha,S_M)\rangle_W.$$

Another approach, is to take the average of the operator A through the propagated states, such as

$$\langle A\rangle = \left\langle\frac{1}{M}\sum_{i=0}^{M-1}A(\alpha(i),S_i)\right\rangle_W.$$

First let us focus on time independent operators and later in time dependent ones.

If A is a diagonal operator in the $\{|\alpha\rangle\}$ basis, and $A|\alpha\rangle = a(\alpha)|\alpha\rangle$, we have that $A(\alpha(i),S_i) = a(\alpha_i)$, so

$$\langle A\rangle = \left\langle\frac{1}{M}\sum_{i=0}^{M-1}a(\alpha(i))\right\rangle_W.$$

For non-diagonal operators, the situation is more complex. In general, A can be written as a sum of Hamiltonian operators H_i, then we can find an expression for the thermal average of A. Let us consider the case where $A = H_k$.

$$\langle A\rangle = \langle H_k\rangle = \frac{1}{Z}\sum_{\alpha}\sum_{S_M}(-1)^{n_2}\frac{\beta^n(M-n)!}{M!}\langle\alpha|H_k\prod_{i=0}^{M-1}S_i|\alpha\rangle$$

Since the operator string is mainly composed of Hamiltonian operators, then it is easy to see that

$$A(\alpha,S_M) = \begin{cases} -n/\beta, & i=k \\ 0 & \text{otherwise}\end{cases}$$

This leads to the number of times the operator H_k appears in the given operator string S_M, defined by $N(k)$.

$$\langle H_k\rangle = -\frac{\langle N(k)\rangle_W}{\beta}.$$

For the case of the total energy the average is given by the mean length of the Hamiltonian operators in the operator string S_M, n. [3]

$$\langle E\rangle = -\frac{\langle n\rangle_W}{\beta}\qquad \langle E^2\rangle = \frac{\langle n(n-1)\rangle_W}{\beta^2}$$

The specific heat is define as the fluctuations in the energy,

$$\langle C\rangle = \beta^2\left[\langle E^2\rangle - \langle E\rangle^2\right] = \langle n^2\rangle_W - \langle n\rangle_W^2 - \langle n\rangle_W.$$

For a product of m operators $H_{k_1},\ldots,H_{k_m}$, we have

$$\left\langle\prod_{i=1}^{m}H_{k_i}\right\rangle = \frac{1}{(-\beta)^m}\left\langle\frac{(n-1)!}{(n-m)!}N(k_1,\ldots,k_m)\right\rangle_W,$$

where $N(k_1,\ldots,k_m)$ is defined as the number of sequences of the order $H_{k_1},\ldots,H_{k_m}$ in S_M. To note that for large operators, this expectation value will be difficult to compute since the probability of them appearing in the SSE operator string is small. In Appendix A the derivation of imaginary-time-dependent operator measurements is presented.

Since the Heisenberg model is a model for magnetism, one might me interested in computing magnetization averages or susceptibilities. The mean magnetization can be written as

$$\langle m\rangle = \frac{1}{M}\sum_{p=1}^{M}\langle\alpha(p)|m|\alpha(p)\rangle,$$

with $m = \frac{1}{N}\sum_{i=1}^{N}S_i^z$. Since the magnetization is a conserved quantity, i.e. $[H,m]=0$, then we may exclude the sum over the propagated states. This way, m is a diagonal operator, so the average magnetization is given by

$$\langle m\rangle = \frac{1}{N}\sum_{i=1}^{N}S_i^z,$$

where S_i^z is defined as the value of the spin, in the z direction, on site i. One might also define the staggered magnetization by $m_s = \frac{1}{N}\sum_{i=1}^{N}\phi_i S_i^z$, where $\phi_i = (-1)^i$. This favours configurations where neighbouring spins alternate value, i.e. anti-parallel configurations. For this case, $[H,m_s]\neq 0$, and then we have to perform the sum over imaginary time as well.

The generalized susceptibility can be written as

$$\chi_{AB} = \left.\frac{\partial\langle A(b)\rangle}{\partial b}\right|_{b=0},$$

where b is the prefactor in a field therm B in the Hamiltonian and A is the operator whose response to this perturbation we want to measure. The most common susceptibility is the magnetic susceptibility, defined as

$$\chi = \left.\frac{\partial\langle m\rangle}{\partial h}\right|_{h=0},$$

[3] Note that to compute the total energy of the system, it is necessary to add the constant C, defined in the Heisenberg Model section. In the specific heat expression the C constants will cancel.

where h is an external magnetic field. This can be written according to a Kubo integral [10](see Appendix A for more information),

$$\chi_{AB} = \int_0^\beta d\tau \langle A(\tau)B(0)\rangle - \beta \langle A\rangle \langle B\rangle .$$

If both A and B are diagonal and commute with the Hamiltonian ($A(p) = A$ and $B(p) = B$), then the susceptibility reduces to the classical expression $\chi_{AB} = \beta(\langle AB\rangle - \langle A\rangle \langle B\rangle)$. For the magnetic susceptibility we have

$$\chi = \beta(\langle m^2\rangle - \langle m\rangle^2).$$

SSE Applied to the Heisenberg Model

Having developed the SSE frame work and rearranging the Heisenberg Hamiltonian, let us apply the SSE method to the Heisenberg model. Since we will just consider a $1D$ chain and $2D$ square lattice, both with periodic boundary conditions, n_2 is even, thus the partition function may be written as

$$Z = \sum_\alpha \sum_{S_M} \frac{\beta^n (M-n)!}{M!} \langle\alpha| \prod_{i=0}^{M-1} H_{a_i,b_i} |\alpha\rangle .$$

S_M now denotes a sequence of indices

$$S_M = [a_0,b_0]_0, [a_1,b_1]_1, \ldots, [a_{M-1},b_{M-1}]_{M-1},$$

where $a_i \in \{1,2\}$ and $b_i \in \{1,\ldots,N_b\}$ denotes an Hamiltonian bond operator H_{a_i,b_i}, or $[a_i,b_i] = [0,0]$ denotes the identity operator I. It is convenient to define the propagate state at some bond b $|\alpha_b(p)\rangle = \left|S^z_{i(b)}(p), S^z_{j(b)}(p)\right\rangle$.

The simulation is started in a random state $|\alpha\rangle$ and an empty operator string, i.e. $S_p = [0,0]_p$. M is chosen arbitrarily and adjusted during the equilibration part of the simulation, leading to no truncation errors. The diagonal updates are carried sequentially for each position $p = 0,\ldots,M-1$ for which $S_p = [0,0]_p$ or $S_p = [1,b]_p$. This type of update changes the expansion power n by ± 1. The acceptance probabilities for the insertion $[0,0]_p \to [1,b]_p$ or removal $[1,b]_p \to [0,0]_p$ of a diagonal operator have to satisfy the detailed balance condition.

$$P([0,0]_p \to [1,b]_p) = \frac{N_b \beta \langle\alpha_b(p)| H_{1,b} |\alpha_b(p)\rangle}{M-n}$$
$$P([1,b]_p \to [0,0]_p) = \frac{L-n+1}{N_b \beta \langle\alpha_b(p)| H_{1,b} |\alpha_b(p)\rangle}$$

Each time an off-diagonal operator is encountered $[2,b]_p$, the state $|\alpha(p)\rangle$ is propagated, i.e. the appropriate spins are flipped due to the action of the off-diagonal operator.

The loop-operator update is a way of sampling off-diagonal matrix elements. It is carried at constant n. For this, it is useful to disregard the $[0,0]_p$ operators in S_M and work with the reduced sequences S_n containing only the Hamiltonian operators $[1,b]_p$ and $[2,b]_p$ (now, $p = 0,\ldots,n-1$). The weight factor is now given by

$$W(\alpha,S_n) = \frac{\beta^n}{n!} \prod_{p=0}^{n-1} \left\langle \alpha_{b_p}(p)\right| H_{b_p} \left|\alpha_{b_p}(p-1)\right\rangle ,$$

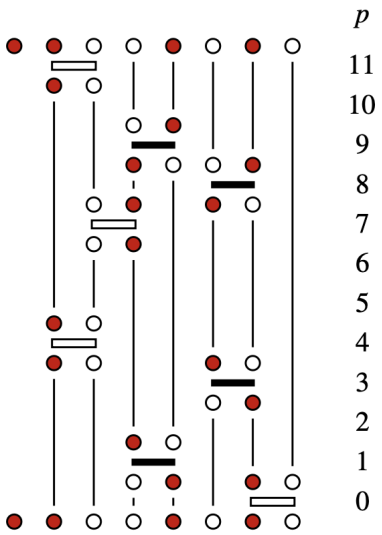

FIGURE 1: Example of SSE configuration represented in a network of connected vertices. Solid and open circles represent spin up and spin down particles, respectively. Taken from [11]

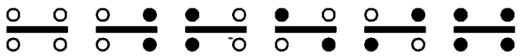

FIGURE 2: All of the possible matrix elements of $W(\alpha,S_n)$ graphically represented. Solid and open circles represent spin up and spin down particles, respectively. The direction of propagation is from below to above. Taken from [3]

where $H_b = H_{1,b} - H_{2,b}$ is the full bond operator. All of the non-zero matrix elements of H_b are

$$\langle\uparrow\uparrow| H_b |\uparrow\uparrow\rangle = \varepsilon + \frac{h}{J};$$
$$\langle\downarrow\downarrow| H_b |\downarrow\downarrow\rangle = \varepsilon;$$
$$\langle\uparrow\downarrow| H_b |\uparrow\downarrow\rangle = \langle\downarrow\uparrow| H_b |\downarrow\uparrow\rangle = \frac{\Delta}{2} + \frac{h}{2J} + \varepsilon;$$
$$\langle\downarrow\uparrow| H_b |\uparrow\downarrow\rangle = \langle\uparrow\downarrow| H_b |\downarrow\uparrow\rangle = \frac{1}{2}.$$

The value of ε is, in principle, arbitrary (but positive). Having a large value for ε may prove counter-productive since the average expansion order increases by $\varepsilon\beta N_b$. It was shown [3], that simulations perform better with finite ε, rather than $\varepsilon = 0$.

These new weights can be graphically represented by a network of n vertices connected to the propagated spins, as shown in Figure 1. All of the possible vertexes are shown in Figure 2. These correspond to all of the non-zero matrix elements. Each p^{th} vertex has two spins $S^z_i(p-1)$ and $S^z_j(p-1)$ entering and two spins $S^z_i(p)$ and $S^z_j(p)$ exiting. For convenience, we can assign legs to each vertex, $l = 0,1,2,3$. In this notation, $l = 0$ represents $S^z_i(p-1)$, $l = 1$ represents $S^z_j(p-1)$, $l = 2$ represents $S^z_i(p)$ and $l = 3$ represents $S^z_j(p)$. This way, we can label the vertex over the propagation direction $p = 0,\ldots,n-1$ as $v = 4p+l$. It

p	v	X(v)	v	X(v)	v	X(v)	v	X(v)
11	44	18	45	30	46	16	47	17
10	40	-	41	-	42	-	43	-
9	36	31	37	7	38	4	39	5
8	32	14	33	15	34	12	35	0
7	28	19	29	6	30	45	31	36
6	24	-	25	-	26	-	27	-
5	20	-	21	-	22	-	23	-
4	16	46	17	47	18	44	19	28
3	12	34	13	2	14	32	15	33
2	8	-	9	-	10	-	11	-
1	4	38	5	39	6	29	7	37
0	0	35	1	3	2	13	3	1
	l=0		l=1		l=2		l=3	

FIGURE 3: Vertex list for the SSE configuration in Figure 1. Taken from [11].

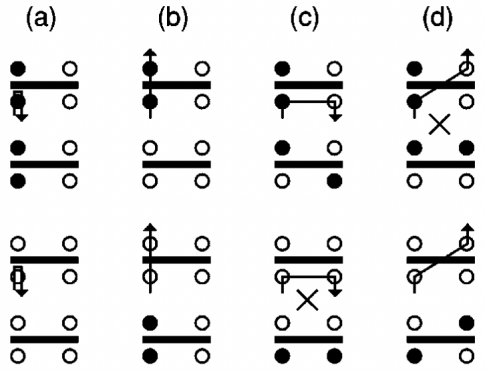

FIGURE 4: All of the paths through two types of vertices given that the entrance leg is $l = 0$. The two cases masked with and X are forbidden, since when the spins are flipped, they generate are not allowed. Taken from [11].

is also useful to keep track of the type of each vertex. So, from Figure 2, we can label the vertex type as 1 through 6, from left to right.

In order co carry out the loop-operator update, we have to construct a doubly-linked list of the vertices. For each of the four legs on each vertex, there is a spin state and a link to the following (same as the propagation direction p) or to the previous (opposite as the direction of propagation p) vertex leg at the same site. The periodic boundary conditions in time have to be satisfied in the construction of said list. An implementation of the construction of the linked list of vertices can be found at [11]. The vertex list for the SSE configuration displayed in Figure 1 is given in Figure 3.

To construct an operator loop, one of the $4n$ legs is chosen at random as the initial entrance leg. One of the four legs belonging to the same vertex is chosen as the exit leg, and both of the spins of the entrance and exit leg are flipped. In Figure 4, examples of how the vertices change in the loop update can be seen. The probabilities of exiting the vertex through a leg given the entrance leg and the vertex type, is proportional to the matrix element of $W(\alpha, S_n)$ (or H_b, since the prefactors cancel) which corresponds to the vertex generated by when the entrance and exit spins are flipped. We can define the matrix element of H_b obtained by flipping spins as

$$W\left(\begin{smallmatrix} f_3, f_4 \\ f_1, f_2 \end{smallmatrix}\right)(p) = \\ = \left\langle f_3 S_i^z(p), f_4 S_j^z(p) \middle| H_b \middle| f_1 S_i^z(p-1), f_2 S_j^z(p-1) \right\rangle,$$

where $f_l = -1$ if the spin at leg l is flipped and $f_l = 1$ if it is unchanged. Then, the probability of, for example, exiting at leg 2, if the entrance leg is 1 is given by

$$P_{2,1} = \frac{W\left(\begin{smallmatrix} + & + \\ - & - \end{smallmatrix}\right)}{W\left(\begin{smallmatrix} + & + \\ + & + \end{smallmatrix}\right) + W\left(\begin{smallmatrix} + & + \\ - & - \end{smallmatrix}\right) + W\left(\begin{smallmatrix} - & + \\ - & + \end{smallmatrix}\right) + W\left(\begin{smallmatrix} + & - \\ - & + \end{smallmatrix}\right)}.$$

The choice and proof of detailed balance for this probability can be seen in [3]. When the spins states are inserted, we have

$$P_{2,1} = \frac{\langle \uparrow\downarrow | H_b | \downarrow\uparrow \rangle}{\langle \downarrow\uparrow | H_b | \downarrow\uparrow \rangle + \langle \uparrow\downarrow | H_b | \downarrow\uparrow \rangle + \langle \uparrow\uparrow | H_b | \uparrow\uparrow \rangle}$$

Then, the chosen exit leg is taken to be entrance leg of the new vertex and the process is repeated. The loop is closed then the original starting point is reached. After this, we update the operator string S_M with information about the new type of operators, since diagonal operators can be flipped to off-diagonal ones and vice-versa. If there are spins on the state $|\alpha\rangle$ that are not acted upon by the operator string S_M, they can not be flipped during the loop-operator update scheme. Thus, after the loop closes, we flip them with $1/2$ probability, since they do not appear in the weight function.

Here we define a Monte Carlo step (MCS) as a full sweep of diagonal updates through all positions of S_M, followed by the construction of the operator list and an N_l of the loop-operator update. During the thermalization/equilibration part of the simulation, we adjust the expansion cut-off M such that if $1.33n > M$, we set the $M \leftarrow 1.33n$. We also update the number of loops N_l such that the total number of visited vertices per MCS is roughly $2M$. After thermalization, we sample the desired quantities.

More about implementation details and program validation can be found at [3, 11]. For more information about procedures on how to measure expectation values, look at [2, 12]

RESULTS AND DISCUSSION

Harmonic Oscillator

For obtaining our results we use the same parameters as Lepage [1]. In other words, we have the lattice spacing

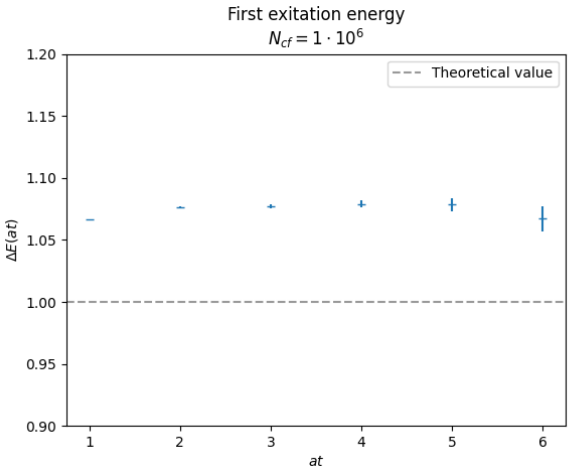

FIGURE 5: Calculated first excitation energy as a function of correlation plotted against the theoretical limit $\Delta E(\infty) = 1$. The errorbars are given by the standard deviation within the 10 bins which constitute the simulation.

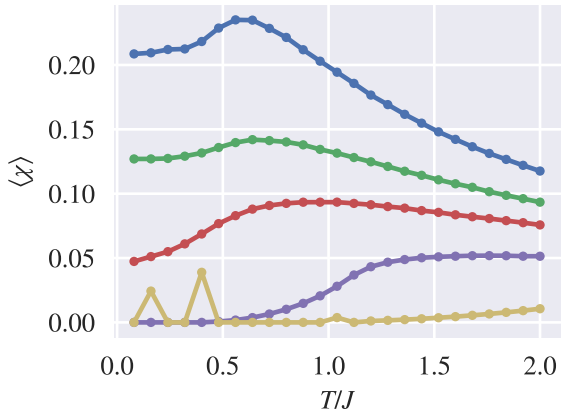

FIGURE 6: Magnetic susceptibility χ as a function of T/J for the zero field Heisenberg model with anisotropy parameter $\Delta = 0, 0.5, 1, 2$ and 4 (top to bottom). In the simulations, 10^6 Monte Carlo cycles with 10 bins were used.

$a = 0.5$ and use natural constants equal to one, $\hbar = \omega = 1$. The number of configurations tested was set to $N_{cf} = 10^6$ and the number of updates before a new sample (in order to minimize correlation) was set to $N_{corr} = 20$. The only other tune-able parameter is ε which puts bounds on the uniform distribution from which the perturbation of the path is chosen. As noted by Lepage [1] the ε should be tuned such that the acceptance rate is between 40% and 60%. By trial and error, an appropriate ε was found to be $\varepsilon = 1.2$ which yielded an acceptance rate of $\sim 55\%$.

In order to compare with Lepage [1] only the first correlations are plotted. The results for a simulation with the specific parameters given above are shown in figure 5.

The first excited energy is calculated to be $\Delta E = 1.06616$, 6.6% off the theoretical answer.

It was found that different simulation configurations resulted in somewhat different values, especially when changing ε and N_{corr}. Other values for the same $\Delta E(at)$'s are given in Table I

Note that the best result is found for $N_{corr} = 100$ and $\varepsilon = 0.9$. This might indicate that despite the equilibration between each measurement, the data could still be somewhat correlated and thus yield some systematic error.

1D Heisenberg chain

For all of the following simulations, to get a better estimation of the error, a procedure called binning was used. We split the Monte Carlo steps in to bins and compute the standard deviation of the mean for all bins. This way, we can get a reasonable estimation of the real standard deviation (standard deviation of the mean).

On Table II, we can see simulational results for the $1D$ isotropic Heisenberg chain with zero field computed by SSE method.

2D Heisenberg lattice

Here we will study more in depth the effects to magnetic anisotropy and external fields on a $2D$ squared lattice with PBC. For all of the simulations, $\varepsilon = 0.25$, so we could have a better sampling without severely affecting the computation time.

Magnetic anisotropy, here represented by the parameter Δ, describes how an object is magnetized differently depending on orientation of the material. This way, there is a preference for the direction of the magnetic moment of the atoms in the material. Here we chose to have a preference along the z axis by multiplying the z operators in the Hamiltonian by the factor Δ.

The magnetic susceptibility for $h = 0$ is shown in Figure 6 for several values of Δ. At lower temperatures, the model with a lower Δ value is more susceptible to external disturbances, such as fields, since this is an energetically more favourable configuration, i.e., the energy of being aligned along the z is lower than any other axis. For larger values of Δ, we see, at lower temperatures, that there is an exponential decay of χ to 0. This reflects a spin gap due to large energy costs of aligning in the z direction. At higher temperatures this spin gap seems to decrease as quantum effects carry less weight.

We can observe the exact same behaviour when we look at the second moment of the staggered magnetization, Figure 7. For lower temperatures, models with a lower Δ parameter are naturally magnetized and as temperature increases the magnetization decreases as well. While for models with larger Δ values, due to the breaking of spin symmetry, we observe no spontaneous magnetization. Furthermore, this result also shows that for lower Δ values, the system behaves like an antiferromagnet at lower T/J and paramagnet at higher T/J.

We now apply an magnetic field h, in the z direction, to the Heisenberg model. This will make our system, at low temperatures, "spontaneously" magnetized, since it is

TABLE I: $\Delta E(at) \pm \sigma$ as a function of N_{corr} and ε when simulated with $N_{cf} = 10^5$ cycles

		at = 1	**at = 2**	**at = 3**	**at = 4**	**at = 5**	**at = 6**
$\mathbf{N_{corr} = 20}$	$\varepsilon = \mathbf{0.6}$	1.06747 ± 0.00251	1.07623 ± 0.00211	1.07940 ± 0.00679	1.08578 ± 0.01216	1.08582 ± 0.01624	1.06618 ± 0.00993
	$\varepsilon = \mathbf{0.9}$	1.06758 ± 0.00231	1.07624 ± 0.00367	1.07936 ± 0.00649	1.08080 ± 0.00852	1.08888 ± 0.01214	1.07515 ± 0.02967
	$\varepsilon = \mathbf{1.2}$	1.06675 ± 0.00180	1.07767 ± 0.00433	1.07879 ± 0.00590	1.08560 ± 0.01087	1.08411 ± 0.01807	1.08534 ± 0.02962
$\mathbf{N_{corr} = 40}$	$\varepsilon = \mathbf{0.6}$	1.06665 ± 0.00207	1.07054 ± 0.00365	1.06748 ± 0.00351	1.07122 ± 0.00940	1.06965 ± 0.01883	1.05218 ± 0.04221
	$\varepsilon = \mathbf{0.9}$	1.06619 ± 0.00243	1.07369 ± 0.00382	1.07486 ± 0.00602	1.07418 ± 0.00692	1.07114 ± 0.01333	1.07525 ± 0.03666
	$\varepsilon = \mathbf{1.2}$	1.06677 ± 0.00132	1.07611 ± 0.00377	1.07594 ± 0.00467	1.07584 ± 0.01029	1.07303 ± 0.01590	1.06051 ± 0.02903
$\mathbf{N_{corr} = 100}$	$\varepsilon = \mathbf{0.6}$	1.06805 ± 0.00154	1.07419 ± 0.00327	1.07458 ± 0.00496	1.07715 ± 0.00516	1.08003 ± 0.01485	1.07675 ± 0.02804
	$\varepsilon = \mathbf{0.9}$	1.06599 ± 0.00129	1.07300 ± 0.00286	1.07377 ± 0.00842	1.07208 ± 0.01307	1.07887 ± 0.01722	1.07080 ± 0.02298
	$\varepsilon = \mathbf{1.2}$	1.06589 ± 0.00136	1.07576 ± 0.00245	1.07593 ± 0.00362	1.07473 ± 0.01010	1.08000 ± 0.01065	1.07258 ± 0.02878

TABLE II: Simulation results for a $1D$ isotropic Heisenberg chain, $L = 128$, with PBC. The standard deviations where obtained through binning the simulation results. A total of 10^6 Monte Carlo steps were used with 10 bins.

T/J	$\langle E \rangle$	C	$\langle m \rangle$	$\langle m^2 \rangle$	$\langle m \rangle_s$	$\langle m^2 \rangle_s$	χ
0.08	-0.4410 ± 0.0001	0.0395 ± 0.0848	0.0000 ± 0.0001	0.0091 ± 0.0001	0.0000 ± 0.0000	1.1848 ± 0.0123	0.1133 ± 0.0011
0.48	-0.3485 ± 0.0002	0.3516 ± 0.0117	0.0000 ± 0.0001	0.0687 ± 0.0006	0.0000 ± 0.0000	0.6259 ± 0.0043	0.1431 ± 0.0013
0.88	-0.2296 ± 0.0003	0.2288 ± 0.0062	0.0000 ± 0.0001	0.1247 ± 0.0004	0.0000 ± 0.0000	0.4578 ± 0.0017	0.1417 ± 0.0005
1.28	-0.1612 ± 0.0003	0.1245 ± 0.0026	0.0001 ± 0.0001	0.1581 ± 0.0006	0.0000 ± 0.0000	0.3863 ± 0.0015	0.1235 ± 0.0005
1.68	-0.1224 ± 0.0003	0.0754 ± 0.0017	0.0000 ± 0.0001	0.1782 ± 0.0010	0.0000 ± 0.0000	0.3515 ± 0.0018	0.1060 ± 0.0006
2.08	-0.0981 ± 0.0003	0.0498 ± 0.0011	0.0000 ± 0.0001	0.1910 ± 0.0006	0.0000 ± 0.0000	0.3324 ± 0.0012	0.0918 ± 0.0003
2.48	-0.0817 ± 0.0004	0.0343 ± 0.0009	0.0001 ± 0.0001	0.2005 ± 0.0010	0.0000 ± 0.0000	0.3205 ± 0.0013	0.0808 ± 0.0004
2.88	-0.0696 ± 0.0004	0.0251 ± 0.0009	0.0000 ± 0.0001	0.2073 ± 0.0008	0.0000 ± 0.0000	0.3142 ± 0.0016	0.0720 ± 0.0003
3.28	-0.0607 ± 0.0005	0.0197 ± 0.0006	0.0000 ± 0.0001	0.2120 ± 0.0007	0.0000 ± 0.0000	0.3081 ± 0.0016	0.0646 ± 0.0002
3.68	-0.0539 ± 0.0005	0.0152 ± 0.0008	0.0000 ± 0.0001	0.2157 ± 0.0011	0.0000 ± 0.0000	0.3035 ± 0.0011	0.0586 ± 0.0003

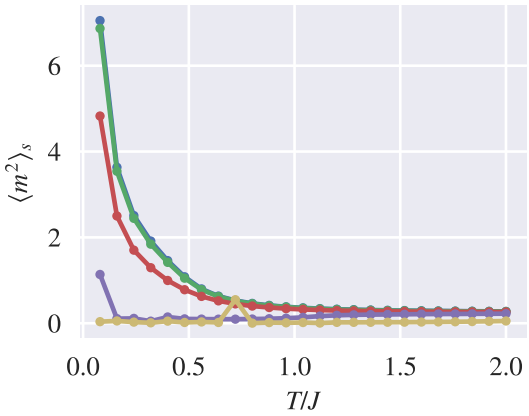

FIGURE 7: Mean squared staggered magnetization $\langle m^2 \rangle_s$ as a function of T/J for the zero field Heisenberg model with anisotropy parameter $\Delta = 0, 0.5, 1, 2$ and 4 (top to bottom). In the simulations, 10^6 Monte Carlo cycles with 10 bins were used.

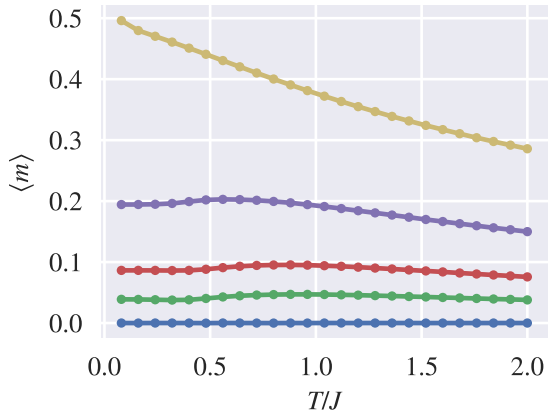

FIGURE 8: Mean magnetization $\langle m \rangle$ as a function of T/J for the isotropic Heisenberg model with applied filed $h/J = 0, 0.25, 0.5, 1$ and 2 (bottom to top). In the simulations, 10^6 Monte Carlo cycles with 10 bins were used.

more energetically favourable to be aligned with the field. The mean magnetization $\langle m \rangle$ for the isotropic Heisenberg model is shown in Figure 8, for different strengths of the applied magnetic field h/J. When there is no applied field, as expected, the mean magnetization is zero, since the spins have perfect symmetry. When we start to disrupt that by applying an external field, it becomes more energetically favourable for the spins to align themselves with the field, thus we observe $\langle m \rangle > 0$. This however is only valid at lower T/J, since at higher T/J, the thermal entropy will take over the system.

CONCLUSION

In conclusion, two Monte Carlo methods were presented, one using the path integral formalism and one using a high-temperature expansion of the partition function.

The results for the path integral which followed the methodology from the notes by Lepage [1] were not identically the same as in the original notes. It was noted by the authors that the translation from python to C++ introduced differences in the calculated values. This could perhaps be due to different random number generators, more research into the matter is necessary. The results from the SSE applied to the Heisenberg model are as expected. We see the expected behaviour of a magnetic model when fields and anisotropies are found. Overall, the implementation of the SSE method works for 1D and 2D systems on bipartite lattices with PBC.

Appendix A: Measuring in SSE: Imaginary-time-dependent product

Now let us consider a imaginary-time-dependent product

$$A_2(\tau)A_1(0) = e^{\tau H}A_2e^{-\tau H}A_1.$$

Taylor expanding the exponentials, the ensemble average can be written as

$$\begin{aligned}\langle A_2(\tau)A_1(0)\rangle &= \frac{1}{Z}\sum_\alpha\sum_{n=0}^{\infty}\sum_{m=0}^{\infty}\frac{(\tau-\beta)^n(-\tau)^m}{n!m!}\langle\alpha|H^nA_2H^mA_1|\alpha\rangle \\ &= \frac{1}{Z}\sum_\alpha\sum_{n=0}^{\infty}\sum_{m=0}^{n}\frac{(\tau-\beta)^{n-m}(-\tau)^m}{(n-m)!m!}\langle\alpha|\prod_{i=m+1}^{n}S_iA_2\prod_{j=1}^{m}S_iA_1,|\alpha\rangle\end{aligned}$$

where in the second transition, we changed the m sum to a sum over the operator string and we sum over all positions of the operator A_2, with n. Considering the first case where A_1 and A_2 are both diagonal operators. If $A_1|\alpha\rangle = a_1(\alpha)|\alpha\rangle$ and $A_2|\alpha\rangle = a_2(\alpha)|\alpha\rangle$, then

$$\langle A_2(\tau)A_1(0)\rangle = \left\langle\sum_{p=0}^{n-1}\sum_{m=0}^{n}\frac{\tau^m(\beta-\tau)^{n-m}}{\beta^n}\frac{(n-1)!}{(n-m)!m!}a_1(\alpha(p))a_2(\alpha(p+m))\right\rangle_W.$$

For non-diagonal operators, let us consider the simplest case where $A_1 = H_{k_1}$ and $A_2 = H_{k_2}$. We get

$$\left\langle H_{k_2}(\tau)H_{k_1}(0)\right\rangle = \left\langle\sum_{m=0}^{n-2}\frac{\tau^m(\beta-\tau)^{n-m-2}}{\beta^n}\frac{(n-1)!}{(n-m-2)!m!}N(k_1,k_2;m)\right\rangle_W,$$

where $N(k_1,k_2;m)$ is defined to be the number of times the operators H_{k_1} and H_{k_2} appear in S_M separated by m steps in imaginary time.

Finally, if we wish to integrate $\langle A_2(\tau)A_1(0)\rangle$ from 0 to β, we are left with a Kubo integral [10]. For the case where A_1 and A_2 are diagonal operators,

$$\int_0^\beta d\tau\,\langle A_2(\tau)A_1(0)\rangle = \left\langle\frac{\beta}{n(n+1)}\left[\left(\sum_{p=0}^{n-1}a_1(\alpha(p))\right)\left(\sum_{p=0}^{n-1}a_2(\alpha(p))\right)+\sum_{p=0}^{n-1}a_1(\alpha(p))a_2(\alpha(p))\right]\right\rangle_W$$

Considering again $A_1 = H_{k_1}$ and $A_2 = H_{k_2}$, we have

$$\begin{aligned}\int_0^\beta d\tau\,\left\langle H_{k_2}(\tau)H_{k_1}(0)\right\rangle &= \frac{1}{\beta}\left\langle\sum_{m=0}^{n-2}N(k_1,k_2;m)\right\rangle_W \\ &= \frac{1}{\beta}\langle N(k_1)N(k_2)\rangle_W.\end{aligned}$$

[1] G. P. Lepage, Lattice qcd for novices 10.48550/ARXIV.HEP-LAT/0506036 (2005).

[2] A. W. Sandvik, A generalization of handscomb's quantum monte carlo scheme-application to the 1d hubbard model, Journal of Physics A: Mathematical and General **25**, 3667 (1992).

[3] O. F. Syljuåsen and A. W. Sandvik, Quantum monte carlo with directed loops, Phys. Rev. E **66**, 046701 (2002).

[4] E. Y. Loh, J. E. Gubernatis, R. T. Scalettar, S. R. White, D. J. Scalapino, and R. L. Sugar, Sign problem in the numerical simulation of many-electron systems, Phys. Rev. B **41**, 9301 (1990).

[5] J. Inácio and D. Aarstein, A variational monte carlo analysis of bose-einstein condensation of trapped bosons github.com/jgci2000/FYS4411-vmc.

[6] D. C. Handscomb, The monte carlo method in quantum statistical mechanics, Mathematical Proceedings of the Cambridge Philosophical Society **58**, 594–598 (1962).

[7] D. C. Handscomb, A monte carlo method applied to the heisenberg ferromagnet, Mathematical Proceedings of the Cambridge Philosophical Society **60**, 115–122 (1964).

[8] A. W. Sandvik, Stochastic series expansion method with operator-loop update, Phys. Rev. B **59**, R14157 (1999).

[9] R. H. Swendsen and J.-S. Wang, Nonuniversal critical dynamics in monte carlo simulations, Phys. Rev. Lett. **58**, 86 (1987).

[10] R. Kubo, Statistical-mechanical theory of irreversible processes. i. general theory and simple applications to magnetic and conduction problems, Journal of the Physical Society of Japan **12**, 570 (1957), https://doi.org/10.1143/JPSJ.12.570.

[11] A. W. Sandvik, A. Avella, and F. Mancini, Computational studies of quantum spin systems, in *AIP Conference Proceedings* (AIP, 2010).

[12] A. W. Sandvik, Finite-size scaling of the ground-state parameters of the two-dimensional heisenberg model, Phys. Rev. B **56**, 11678 (1997).